Elastic and Inelastic Scattering of 28-Mev Deuterons*

R. J. SLOBODRIAN
Synchrocyclotron Laboratory, Nuclear Physics Division, Physics Department, Comisión Nacional de Energía Atómica, Buenos Aires, Argentina

(Received January 10, 1961; revised manuscript received October 23, 1961)

Natural lithium, polyethylene, and aluminum targets were bombarded with 28-Mev deuterons. The outgoing particles were analyzed with a scintillation spectrometer. The angular distributions for the following processes were measured: $Li(d,d)Li$, $Li^7(d,d')Li^{7*}$—4.61 Mev, $C^{12}(d,d)C^{12}$, $C^{12}(d,d')C^{12*}$—4.43 Mev, $Al^{27}(d,d)Al^{27}$, $Al^{27}(d,d')Al^{27*}$—2.21 Mev, and $H^1(d,p)H^2$. The $Li^7(d,d')Li^{7*}$ 4.61-Mev angular distribution can be fitted by superimposing plane-wave direct-reaction curves corresponding to $l=0$, $a=3.4$ f and $l=2$, $a=3.9$ f, where a is the interaction radius and l the angular momentum change; this leads to an odd parity assignment for the level. The angular distribution of the reaction $C^{12}(d,d')C^{12*}$—4.43 Mev is fitted by superimposing the curves of $l=0$, $a=4.1$ f and $l=2$ with $a=4.6$ f. The $Al^{27}(d,d')Al^{27*}$—2.21 Mev angular distribution is adequately fitted with a curve of $l=1$, $a=5.1$ f; therefore there follows an odd parity assignment for the level. The possible spin assignments of the levels are discussed. The inelastic scattering curves yield some evidence of a total spin flip of the deuteron in the reaction. The elastic scattering angular distributions show the usual diffraction pattern, and interaction radii were calculated using an optical analogy that implies the scattering of waves from a black disk. The angular distribution of the interaction $H^1(d,p)H^2$ is consistent with measurements performed at neighboring energies and it also agrees with the curve obtained with a Serber-type force.

I. INTRODUCTION

IN the realm of charged-particle reactions, angular distributions of deuteron-induced reactions have played an important role, mainly since stripping theory provided a tool for the determination of relative parity and spin values of nuclear levels, when the reaction proceeds through a direct process with a forwardly peaked curve. Contrariwise, compound nucleus processes through a single level or through many levels in the continuum region, usually yield angular distributions that are symmetric about 90° in the center-of-mass system, thus inhibiting any conclusion about level properties. Recently, Lane and Thomas have shown that the R-matrix formalism covers all nuclear reactions and that there is no clear-cut difference between both types of processes.[1] The experimental evidence supports their point of view as there are angular distributions that can be interpreted as partly due to a direct process and partly due to compound nucleus formation.[2] The existing data on deuteron reactions reach up to 24 Mev, and at this energy, they are very scant.[3] There is no systematic set of data on the elastic scattering at that energy, nor at higher energies, that would permit an optical model analysis. The same happens with the inelastic scattering between 22 and 28 Mev. The present investigation with 28-Mev deuterons was undertaken to start a survey on light and medium light elements, in order to obtain the interaction parameters and also some additional information on the level properties of the elements involved in the inelastic scattering.

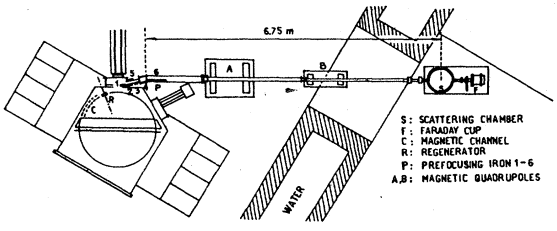

FIG. 1. General view of the external beam facilities of the Buenos Aires 180-cm synchrocyclotron.

II. EXPERIMENTAL PROCEDURE

A. Machine and External Beam Facilities

The 28-Mev deuteron source was the Buenos Aires 180-cm synchrocyclotron. The external beam facilities are shown in Fig. 1 and have been described elsewhere up to the scattering chamber.[4,5] The latter is 54 cm in diameter and has fixed windows on short tubes every 5° on two opposite quadrants, covering the angles from 10° to 170°. At 90° there are five overlapping positions and 15° can be measured on either side of the beam to check the beam position. The windows are covered with thin duraluminum foil and the chamber is supported on

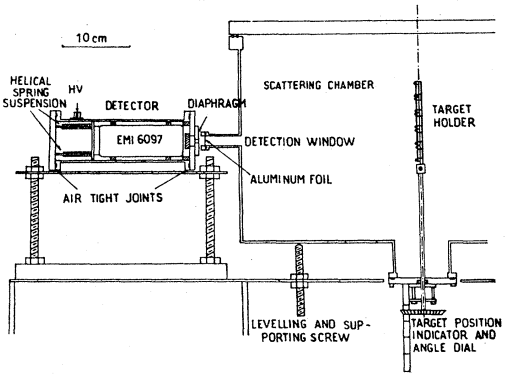

FIG. 2. Schematic drawing showing the detector geometry and the scattering chamber (side view).

* Based on communications to the Asociación Física Argentina during the following meetings; XXXIV, September, 1959, XXXV, May, 1960, and XXXVI, September, 1960 (unpublished).

[1] A. M. Lane and R. G. Thomas, Revs. Modern Phys. **30**, 257 (1958).

[2] Homer E. Conzett, Phys. Rev. **105**, 1324 (1957).

[3] Robert G. Summers-Gill, Phys. Rev. **109**, 1591 (1958).

[4] P. A. Lenk and R. J. Slobodrian, Phys. Rev. **116**, 1229 (1959).

[5] J. Rosenblatt and R. J. Slobodrian, Rev. Sci. Instr. **31**, 863 (1960).

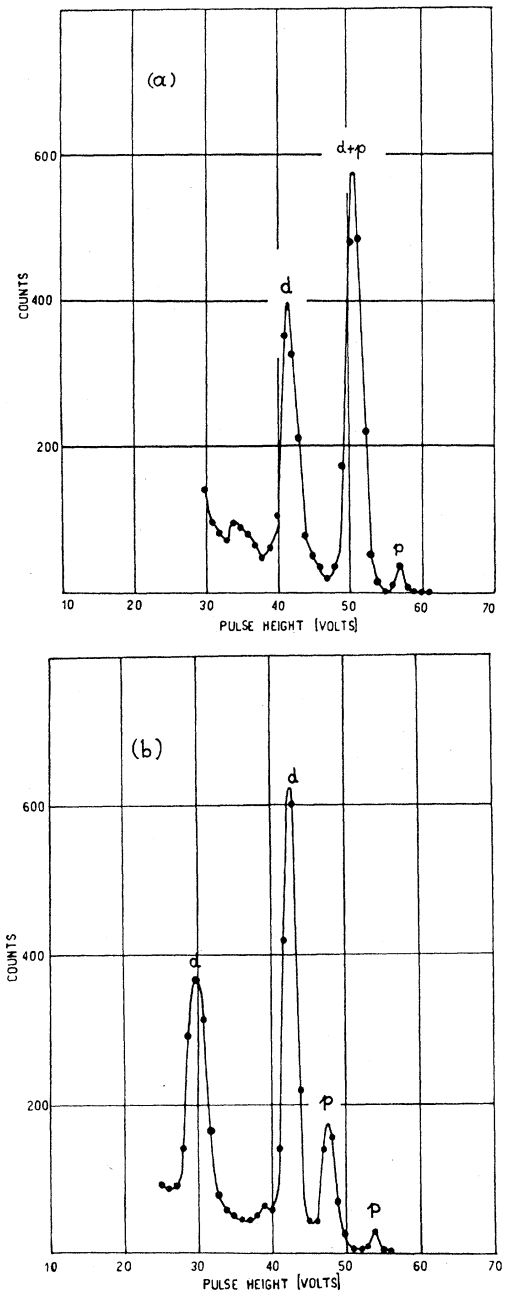

FIG. 3. (a) Charged particle spectrum from carbon at $\theta_{lab}=70°$. (b) The same spectrum taken with 98 mg/cm² in front of the scintillator.

three screws that permit leveling. The target holder can bear five different targets and can be rotated from the outside. The target position can be assured down to $\pm 0.25°$. The detector is placed in the open air in front of the windows and its position is known to within $\pm 0.2°$. The chamber also permits work with nonpressurized gaseous targets, placing a set of collimators inside the window tubes. The chamber is shown in Fig. 2. No collimators are used to define the beam size, that is of the order of 0.5 cm². A Faraday cup with remotely controlled absorber wheels permits the beam energy measurement and also an indirect determination of the target thickness.[2]

B. Particle Detection and Beam Monitoring

The particle detection and spectrometry was achieved with NaI(Tl) and CsI(Tl) crystals, a phototube (EMI 6097), and a single-channel pulse-height analyzer. The detector geometry is shown in Fig. 2. The operation with NaI(Tl) required particular care to avoid crystal hydration. This was prevented by sealing the crystal mounted on Lucite with a thin aluminum foil and heavy silicone oil. The detector enclosure was air tight and it included small sacks with silica gel. The carbon and hydrogen data were taken with the NaI(Tl) crystal without any appreciable change in resolution, and when it was taken out there was no significant hydration. The identification of the scattered particles was obtained with the help of kinematics and also by using aluminum absorbers in order to determine the energy loss of the different groups of particles, with a given thickness of absorber. The last mentioned procedure was also used to separate superimposed groups of particles. This laborious but simple particle identification and separation method is illustrated in Fig. 3. The optimum resolution was of the order of 2.2% for particle groups around 28 Mev.

A block diagram of the electronics and the beam monitoring system is shown in Fig. 4. The charge collector is a Faraday cup with its bottom lined with a thick disk of graphite; it is provided with a permanent magnet to avoid loss of secondaries. The cup is insulated with Lucite and is mounted inside the cylinder shown in Fig. 1. The beam current is integrated on calibrated condensers and measured with a negative-feedback electrometer and a Speedomax recording voltmeter. The system includes a recycling device that permits a wide range of preset total charge values, in conjunction with different capacitors in the electrometer. The recycling system permits the choice of one to fifteen cycles, and gates simultaneously the scaler of the spectrometer. The beam current can be measured with the same electrometer, using adequate resistors, thus permitting the beam range on aluminum to be determined and also an easy tuning of the machine on maximum external beam.

C. Targets

The lithium target was prepared by rolling the chemically pure element under petroleum ether and then transferred quickly to the target holder position in the scattering chamber, previously filled with nitrogen. The lithium target was kept wet with petroleum ether until the lid was placed on the chamber; the latter was evacuated immediately afterwards. The spectra obtained with lithium targets prepared in this manner did not show any appreciable contamination with C, O, or

H. The target thickness measurement was performed as described by Conzett.[2]

The polyethylene target was a commercially available 1.85-mg/cm² foil. The aluminum target was 9.50 mg/cm² thick and was at least 99.7% pure, as established by spectrographic analysis.

D. Errors and Experimental Uncertainties

The beam energy is presently known to within 1% due to the uncertainty in the thickness of the aluminum foils used for the range measurement. On the other hand, the beam energy spread was found to be less than 0.2%.[4] The beam energy is also very stable with little precaution on the parameters of the deflector and the magnetic field of the machine. No drift was observed down to 0.4% in energy. The beam current integration error is of the order of 1%. The error in solid angle is 1.5%. The incident beam spread is of the order of 1° and the detector acceptance angle varied between 0.8° and 1.2° for different detector windows. No corrections were done for this finite geometry because they are negligible compared with the other uncertainties.

The peaks shown in Figs. 3, 5, and 8, were usually integrated and the differential curve was used mainly for background subtraction. Window widths of 1, 2, 5, and 10 v as well as discriminator setting are available on the spectrometer. The 10-v window was the more commonly used for the integration; a cross-check was always performed by taking the number of counts on discriminator at the beginning and at the end of the window, and comparing the difference with the window result. Generally speaking the main source of experimental error was the background subtraction.

The scintillator particle detection efficiency was taken equal to one as it was reasonable to expect that all particles accepted by the defining apertures were counted.

III. RESULTS AND CONCLUSIONS

A. General

Figures 6, 7, and 9 through 13 contain the experimentally determined absolute differential cross sections referred to the center-of-mass system; the conversion was effected by means of tables due to Marion *et al.*[6] The inelastic process angular distributions are accompanied by the direct-reaction theoretical curves, using the plane wave undistorted form of the theory. The elastic scattering curves are shown together with the Rutherford differential cross section and the ratio to it. The relative errors are indicated on the curves as they are the ones to define the shape of the angular distribution.

The number of levels of the compound nucleus involved with an energy spread of 56 kev for the incident deuterons was calculated using the usual expression of

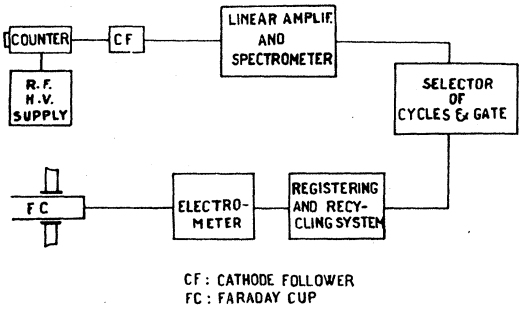

FIG. 4. Block diagram of the electronics and the beam monitoring system.

the level density,

$$w(E)=C\exp[2(aE)^{\frac{1}{2}}], \tag{1}$$

where E is the excitation energy, C and a are constants (see Blatt and Weisskopf[7]). The cross section for the formation of the compound nucleus was estimated with the asymptotic expression

$$\sigma_c\simeq\pi(R+\lambda)^2[1-V(R+\lambda)/E], \tag{2}$$

where λ is the "de Broglie" wavelength of the projectile divided by 2π, R is the reaction channel radius, E is the center-of-mass energy of the projectile, and V is the Coulomb potential. Table I condenses the results of the calculations. In the case of the lithium target, its thickness being some 450 kev, the total number of levels of the compound nucleus involved is much larger; the

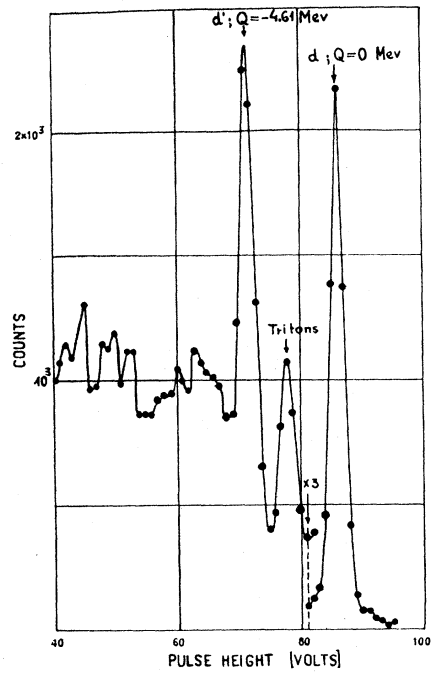

FIG. 5. Charged particle spectrum from lithium at $\theta_{lab}=35°$.

[6] J. B. Marion, T. I. Arnette, and H. C. Owens, Oak Ridge National Laboratory Report ORNL-2574 (unpublished).

[7] J. M. Blatt and V. F. Weisskopf, *Theoretical Nuclear Physics* (John Wiley & Sons, Inc., New York, 1952).

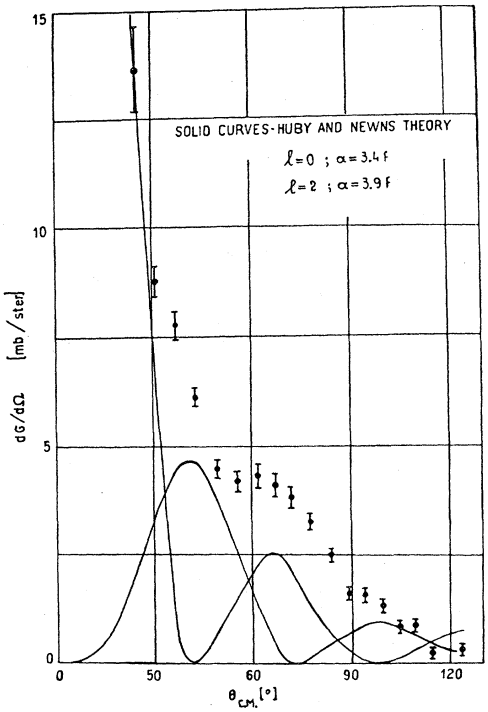

FIG. 6. Angular distribution of deuterons from the reaction $Li^7(d,d')Li^{7*}$ 4.61 Mev.

same happens with aluminum. Table I includes, therefore, a column that takes into account the number of levels involved due to the finite target thickness.

All the angular distributions due to inelastic scattering of the incident deuterons were fitted using the Huby and Newns theory,[8] that is with spherical Bessel functions. Nevertheless it is worth while to mention that using the semiclassical approach of Butler *et al.*,[9] it is possible to obtain a reasonable fit. The Huby and Newns differential cross section is given by

$$\frac{d\sigma}{d\Omega}=\sum_l |A_l|^2\left[\frac{4\alpha}{k}\arctan\frac{k}{4\alpha}j_l(ka)\right]^2, \qquad (3)$$

TABLE I. Excitation energy of the compound nucleus using deuterons as projectiles, cross section for the formation of the compound nucleus calculated with the asymptotic expression (2), and number of levels of the compound nucleus involved in the reaction due to the spread in energy of the incident beam and to the finite target thickness, calculated with expression (1).

Element	Excitation energy (Mev)	Cross section (mb)	Number of levels (infinitely thin target)	Number of levels (thick target)
Lithium	38.4	750	11	105
Carbon	34.3	884	30	54
Aluminum	43.9	1,100	340	1,700

[8] R. Huby and H. C. Newns, Phil. Mag. **42**, 1442 (1951).
[9] S. T. Butler, N. Austern, and C. Pearson, Phys. Rev. **112**, 1227 (1958).

where $k=[(k_i-k_f)^2+4k_ik_f\sin^2\theta/2]^{\frac{1}{2}}$, k_i and k_f are the initial and final wave numbers, respectively, $\alpha=(M_nE_b)^{\frac{1}{2}}/\hbar$, the deuteron wave-function relaxation length being $1/\alpha$, the A_l's are constants, a is the "interaction radius" and $j_l(ka)$ is a spherical Bessel function, M_n is the average nucleon mass, and E_b is the deuteron binding energy.

The angular distribution of the elastically scattered deuterons were analyzed using a simple optical analogy[3–10] in order to obtain the deuteron nucleus interaction radii. The elastic scattering cross section, obtained by considering the scattering of the particle associated waves by a black disk, is given by

$$d\sigma_{el}/d\Omega\simeq R^2\{J_1^2[2kR\sin(\theta/2)]/4\sin^2(\theta/2)\}, \qquad (4)$$

where k is the wave number of the scattered particle, R is the interaction radius, and J_1 is the first-order Bessel function. The "black disk" approximation neglects Coulomb scattering, and therefore it should yield better results when the ratio of the observed cross section to Rutherford is large.

B. Angular Distributions Due to Inelastic Scattering

1. $Li^7(d,d')Li^{7*}$ 4.61-Mev Level

A typical spectrum is shown in Fig. 5. Besides the group of elastically scattered deuterons and the inelastic group corresponding to the excitation of the 4.61-Mev level, there is a triton group belonging to the reaction

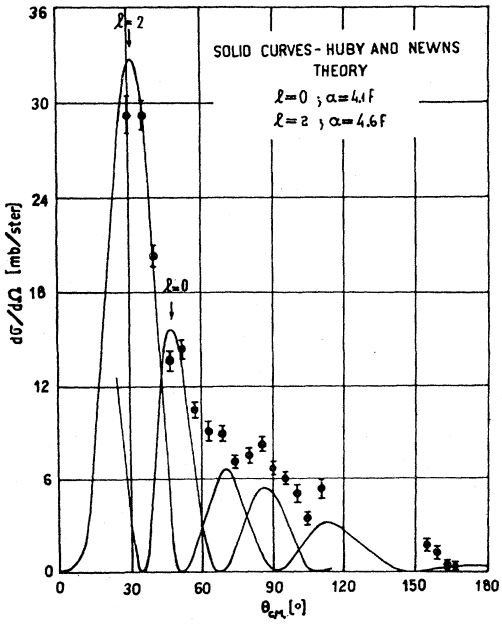

FIG. 7. Angular distribution of deuterons from the reaction $C^{12}(d,d')C^{12*}$ 4.43 Mev.

[10] R. M. Eisberg, G. Igo, and H. E. Wegner, Phys. Rev. **99**, 1606 (1955): R. G. Summers-Gill, University of California Report, UCRL-3388 (unpublished).

$Li^7(d,t)Li^6$ and its angular distribution was also obtained; it will be reported in another paper.

The angular distribution of the deuterons corresponding to the $Li^7(d,d')Li^{7*}$ 4.61-Mev reaction is shown in Fig. 6; a good fit of the experimental data can be obtained by superimposing the theoretical curves[8] with $l=0$, $a=3.4$ f, and $l=2$, $a=3.9$ f; they are drawn separately for the sake of clarity. Earlier work on this level was performed by various authors.[2–11] The angular distributions obtained by Levine *et al.* in Pittsburgh using 14.8-Mev deuterons, either by stripping on Li^6 or by inelastic deuteron scattering on Li^7, were almost isotropic and no conclusions concerning the level properties could be drawn. Haffner's results obtained with 15-Mev deuterons showed instead a forwardly peaked angular distribution,[11] and it was fitted with a direct reaction curve of $l=1$. Conzett[2] studied this level with 12-Mev protons and obtained a curve that had a strong compound nucleus contribution. The experimental results could be fitted by superimposing a curve symmetrical with respect to 90° and a direct reaction curve of $l=0$. Conzett's assignments of spin and parity are $J=\frac{1}{2}$, $\frac{3}{2}$, or $\frac{5}{2}$, and odd parity. Makaryunas and Starodubtsev[11] excited this level with 13.2-Mev alpha particles and obtained a predominantly direct reaction curve corresponding to $l=2$. Their assignments are $J=\frac{1}{2}$, $\frac{3}{2}$, $\frac{5}{2}$, and $\frac{7}{2}$ and odd parity. Present results, taking into account considerations given at length by Conzett[2] and Summer-

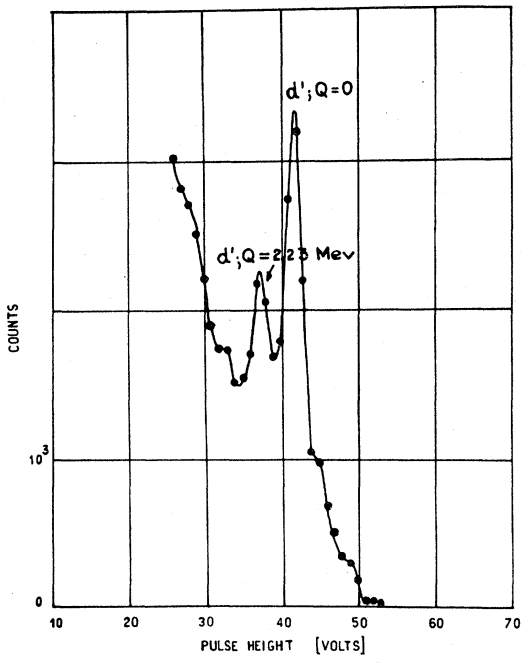

FIG. 8. Charged particle spectrum from aluminum at $\theta_{lab}=85°$.

[11] S. H. Levine, R. S. Bender, and J. N. Mc Gruer, Phys. Rev. **97**, 1249 (1955): J. W. Haffner, *ibid.* **103**, 1398 (1956): E. W. Hamburger and J. R. Cameron, *ibid.* **117**, 781 (1960): K. V. Makaryunas and S. V. Starodubtsev, Soviet Phys. JETP **11**, 271 (1960).

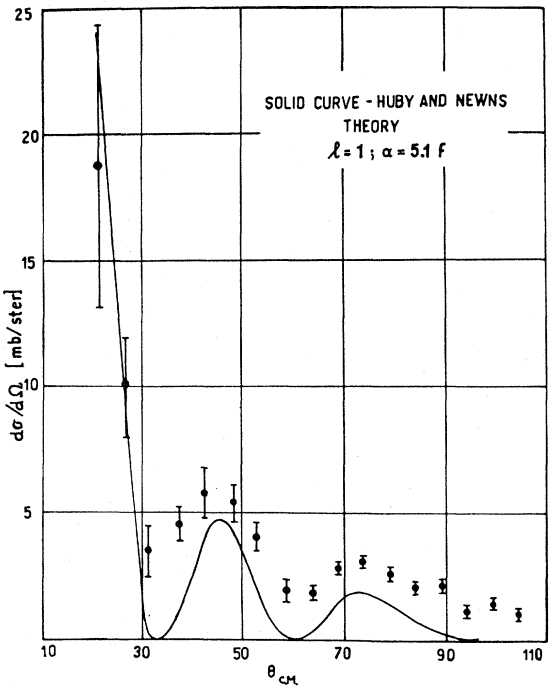

FIG. 9. Angular distribution of deuterons from the reaction $Al^{27}(d,d')Al^{27*}$ 2.21 Mev.

Gill,[10] imply for the $l=0$ contribution $J=\frac{3}{2}$ and odd parity, whereas the $l=2$ contribution implies $J=\frac{1}{2}$, $\frac{3}{2}$, $\frac{5}{2}$, $\frac{7}{2}$, and odd parity. The selection rules are simply

$$|J_i+J_f|\equiv\Delta J=l \quad \text{and} \quad \Pi_i\Pi_f=(-1)^l, \qquad (5)$$

in terms of the spins and parities of the initial and final states of the target nucleus. The $l=2$ value is in agreement with the $J=\frac{7}{2}^-$ prediction of the shell model.[12] Nevertheless one could imagine that if the deuteron interacts as a whole, and not only through one of its nucleons, it could flip its spin, and then the angular momentum rule should be $\Delta J=l, l\pm2$. In that case both l values would yield the same set of possible final spin J_f values, excluding the unusually high $\Delta J=4$ spin change. The general conclusion is that the parity of the level seems to be odd, and that the shell-model prediction is not in disagreement with the experimental results if one assumes a total spin flip of the deuteron.

2. $C^{12}(d,d')C^{12*}$ 4.43-Mev Level

Some typical spectra are shown in Fig. 3. The particle groups correspond to elastically scattered deuterons, to the inelastic scattering on the 4.43-Mev level, and to the stripping reactions $C^{12}(d,p)C^{13}$, and $C^{12}(d,p)C^{13*}$ 3.68-Mev. The stripping reactions angular distributions will be reported in another paper. The 4.43-Mev level of C^{12} is known to be a 2^+ state and the ground state is 0^+. Therefore $\Delta J=2$ and there should be no parity change.

[12] D. R. Inglis, Revs. Modern Phys. **25**, 390 (1953): D. Kurath, Phys. Rev. **101**, 216 (1956).

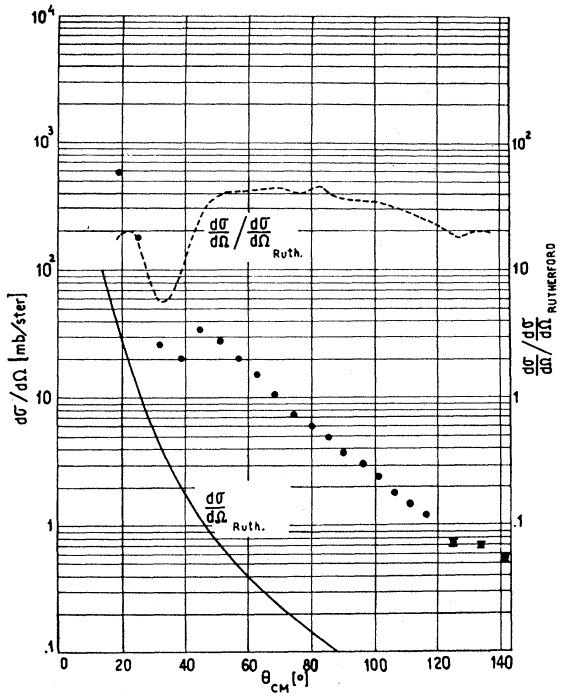

FIG. 10. Angular distribution of deuterons elastically scattered from lithium.

The $l=2$ direct reaction curve for $a=4.6$ f follows the general trend of the experimental angular distribution. Nevertheless, here again a better fit of the experimental data can be obtained if one adds the $l=0$ curve with $a=4.1$ f. Both theoretical curves are drawn separately in Fig. 7 but it is easy to see that a superposition of both would give account of the oscillations of the experimental distribution. The same level excited with 12-Mev protons[2] did not yield any agreement with direct interaction theory, instead it showed a strong compound nucleus contribution. Something analogous happens when the level is excited with protons between 14.7 and 19.4 Mev.[13] The data obtained in this experiment imply an almost pure direct interaction of the deuteron with the carbon nucleus. The fact that a better agreement is obtained including the $l=0$ curve would mean, taking as unshakable the 2^+ assignment for the 4.43-Mev level, that there is a complete flip of the deuteron spin, and then, here again the angular momentum selection rule should be $\Delta J=l$, $l\pm2$, thus permitting the $l=0$ value.[14]

3. $Al^{27}(d,d')Al^{27*}$ 2.21-Mev

A typical spectrum is shown in Fig. 8. The angular distribution corresponding to the reaction $Al^{27}(d,d')Al^{27*}$ 2.21-Mev is shown in Fig. 9. It was fitted with a direct interaction curve of $l=1$ and $a=5.1$ f. The Al^{27} ground-state spin is $\frac{5}{2}$ and the parity is even. Therefore, according with the selection rules (5), the 2.21-Mev level should have $J=\frac{3}{2}$, $\frac{5}{2}$ or $\frac{7}{2}$ and odd parity. In this case there is a remarkably good agreement of the experimental results with a single theoretical curve, that is with a single l value. The Al^{27} nucleus cannot be reached by means of (d,p) or (d,n) reactions on naturally occurring nuclei. The information concerning its levels is due mainly to $\beta-\gamma$ spectroscopy. The present parity assignment agrees with Haffner's results[11] and disagrees with the results of Hinds and Middleton.[15] The particle spectra obtained in this experiment show a fast rising background. This is probably due to the multiple reactions that can take place at the high-excitation energies of the compound nucleus.

C. Angular Distributions of the Elastic Scattering on Li, C, and Al

The elastic scattering curves are shown in Figs. 10–12, together with the Rutherford cross section. The ratio to Rutherford cross section is also shown. The curves exhibit the typical diffraction pattern common to other particles and similar to the curves obtained at lower energies.[3–16] The curve obtained from lithium presents a single distinct oscillation. This may be due to the obscuring effect of Li^6 in the interference phenomenon. In fact the deuteron wave number is some 20% smaller

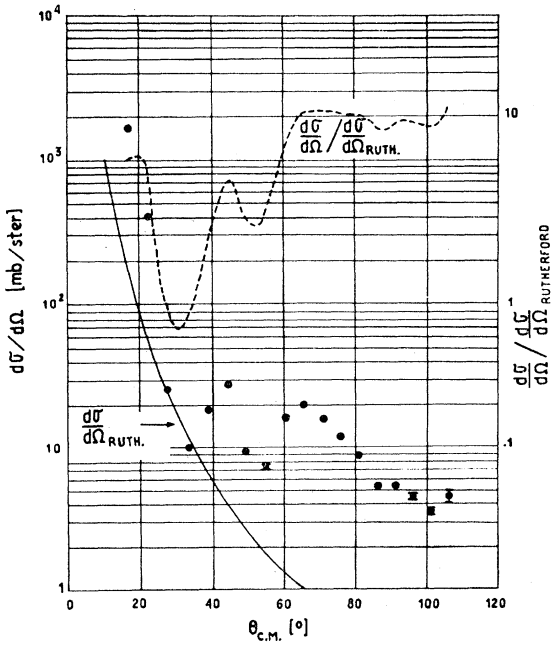

FIG. 11. Angular distribution of deuterons elastically scattered from carbon.

[13] Robert W. Peelle, Phys. Rev. **105**, 1311 (1957).

[14] The author is aware that the information contained in sections B. 1. and B. 2. is not a conclusive proof of the deuteron spin flip. It is interesting to note that the deuteron could also reorient its spin in the interaction yielding $\Delta J=l\pm1$.

[15] S. Hinds and R. Middleton, Proc. Phys. Soc. (London) **A69**, 347 (1956).

[16] G. E. Fischer and V. K. Fischer, Phys. Rev. **114**, 533 (1959); J. L. Yntema, *ibid.* **113**, 261 (1959).

TABLE II. Interaction radii obtained by diffraction analysis of the elastic scattering of 28-Mev deuterons.

Element	Maxima (deg)	Minima (deg)	Interaction radius (f)	Average interaction radius (f)
Lithium		36	4.1	4.1
		75		
Carbon	43		6.82	7.0
	63			
		32	7.14	
		52		
Aluminum	36		7.3	
	54		7.6	
	72			7.3
		30	7	
		47	7.3	
		73		

for Li^6 than for Li^7 and this shifts the oscillations of the angular distribution to higher scattering angles, washing out the diffraction structure. The angular distributions of C and Al are normal. A simple analysis of the diffraction pattern has been carried out through the use of expression (4), because the spacing between adjacent maxima (or minima) of the cross section is approximately π. The interaction radius R can be obtained simply as

$$R=\pi/\{2k[\sin(\theta_{i+1}/2)-\sin(\theta_i/2)]\}, \qquad (6)$$

where k is the wave number of the scattered particles, θ_i is the angle where the ith maximum is observed; a similar equation applies for the minima. Table II condenses the information obtained by means of this analysis. Maintaining the nuclear radius as

$$R=1.3A^{\frac{1}{3}}\text{ f}, \qquad (7)$$

the result obtained from lithium implies that the interaction radius of the deuteron is 1.6 f. The deuteron radius calculated from (7) is 1.64 f. Instead the data from carbon and aluminum yield much larger interaction radii: 4 f and 3.4 f, respectively. Both values lie close to 4.31 f, obtained from

$$\rho=\hbar/(M_nE_b)^{\frac{1}{2}}, \qquad (8)$$

where M_n and E_b have the same meaning as in α of expression (3), ρ is the relaxation length of the deuteron radial wave function.[17] The center-of-mass energy of the incident deuterons is 21.8 Mev for lithium, 24 Mev for carbon, and 26 Mev for aluminum. This is of little importance if the parameters obtained from the experiment are energy independent. When such a dependence exists or is suspected the ideal experimental conditions should imply a change in laboratory energy for each element in order to keep constant the center-of-mass energy, thereby permitting the comparison of the results obtained for different nuclei.

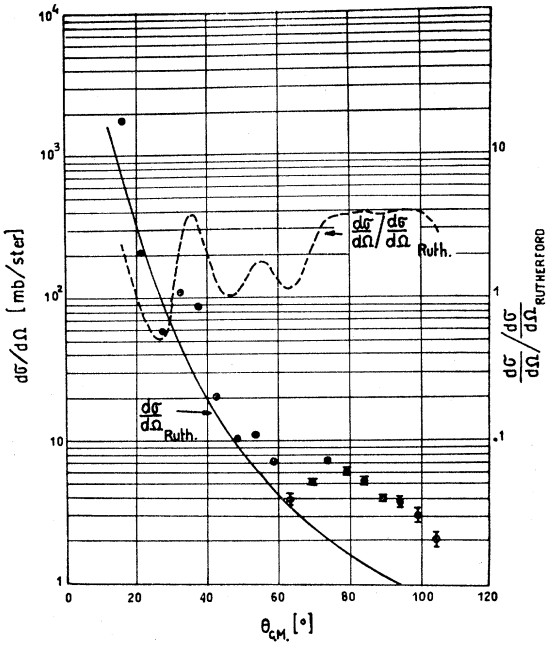

FIG. 12. Angular distribution of deuterons elastically scattered from aluminum.

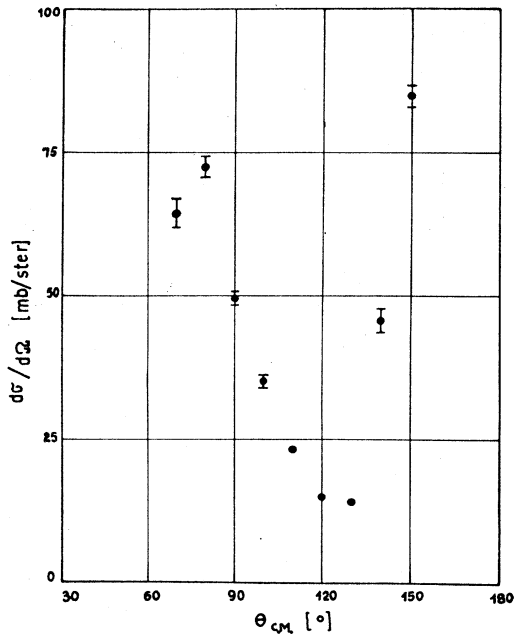

FIG. 13. Angular distribution of the interaction $H^1(d,p)H^2$.

D. Deuteron-Proton Interaction

The angular distribution of the interaction $H^1(d,p)H^2$ is shown in Fig. 13. The energy available for the interaction is 9.3 Mev because 18.8 Mev are carried by the center of mass. The data reported here are consistent

[17] Robley D. Evans, *The Atomic Nucleus* (McGraw-Hill Book Company, Inc., New York, 1955).

with the results of other experiments; they correspond to an intermediate energy between Rotblat's and Caldwell and Richardson's data.[18] As is well known,[19] the deuteron-proton interaction in this energy range is well represented by a Serber force, and this is confirmed at the interaction energy of 9.3 Mev.

E. Conclusions

Due to the high-excitation energy of the compound nucleus (Table I), multiple reactions are favored and there are many competing channels, therefore the incident particle reemission is not likely to occur. It is then logical that simple reactions would proceed through a direct type of mechanism. The particle spectra reported here were measured up to 165° in the laboratory system, although the plots of the cross section as a function of angle were interrupted when the error became unreasonably large. Nevertheless the angular distributions corresponding to inelastic deuteron scattering did not show a rise for large scattering angles. There is undoubtedly a very slight contribution due to compound nucleus formation, if any. The $X(d,d')X$ cross sections are rather high taking into account that the deuteron is a loosely bound structure and would more likely break up than interact as a whole. The tentative explanation of the appearance of two l values in order to fit the experimental structure of the angular distribution, as due to the total spin flip of the deuteron, seems to indicate that it really interacts as a whole. Otherwise, it would be hard to explain a total spin flip with a significant cross section. The elastic scattering angular distributions will be submitted to an optical model analysis with an electronic computer in the future. The interaction radii contained in Table II could be used directly in the asymptotic expression (2) instead of $R+\lambda$, yielding perhaps a more realistic value of σ_c. On the other hand they can be useful as a starting point for the machine computations.

[18] J. Rotblat, *Proceedings of the 1954 Glasgow Conference on Nuclear and Meson Physics* (Pergamon Press, New York, 1955). D. O. Caldwell and J. R. Richardson, Phys. Rev. **98**, 28 (1955).

[19] A. H. de Borde and H. S. W. Massey, Proc. Phys. Soc. (London) **A68**, 769 (1955).

ACKNOWLEDGMENTS

It is a pleasure to thank electronics engineer P. A. Lenk for the design and construction of several circuits and the recycling system; the synchrocyclotron technicians J. Garanzini, B. Ietri, M. Professi, and S. Tejero, for their invaluable help during the experiment; Dr. Homer E. Conzett of the Lawrence Radiation Laboratory who kindly gave us the CsI(Tl) crystals; Dr. D. R. Bès and Dr. S. Mayo for useful discussions during the preparation of the manuscript. The author wishes to express his gratitude to the staff members of the University of California Radiation Laboratory who made possible his fruitful two-years stay (1955 to 1957) at the Laboratory, and helped, thereby, the development of the nuclear reactions program with the Buenos Aires synchrocyclotron. It is a distinct pleasure to thank particularly Professor Robert Thornton, Professor Emilio Segrè, and Professor A. C. Helmholz.